Heterologous prime-boost vaccination targeting MAGE-type antigens promotes tumor T-cell infiltration and improves checkpoint blockade therapy

James McAuliffe,[1] Hok Fung Chan,[1] Laurine Noblecourt,[1]
Ramiro Andrei Ramirez-Valdez,[1] Vinnycius Pereira-Almeida,[1,2] Yaxuan Zhou,[1,3]
Emily Pollock,[4] Federica Cappuccini,[4] Irina Redchenko,[4] Adrian VS Hill,[4]
Carol Sze Ki Leung ![ORCID],[1] Benoit J Van den Eynde ![ORCID] [1,5]

ABSTRACT

Background The clinical benefit of immune checkpoint blockade (ICB) therapy is often limited by the lack of pre-existing CD8+ T cells infiltrating the tumor. In principle, CD8+ T-cell infiltration could be promoted by therapeutic vaccination. However, this remains challenging given the paucity of vaccine platforms able to induce the strong cytotoxic CD8+ T-cell response required to reject tumors. A therapeutic cancer vaccine that induces a robust cytotoxic CD8+ T-cell response against shared tumor antigens and can be combined with ICB could improve the outcome of cancer immunotherapy.

Methods Here, we developed a heterologous prime-boost vaccine based on a chimpanzee adenovirus (ChAdOx1) and a modified vaccinia Ankara (MVA) encoding MAGE-type antigens, which are tumor-specific shared antigens expressed in different tumor types. The mouse MAGE-type antigen P1A was used as a surrogate to study the efficacy of the vaccine in combination with ICB in murine tumor models expressing the P1A antigen. To characterize the vaccine-induced immune response, we performed flow cytometry and transcriptomic analyses.

Results The ChAdOx1/MVA vaccine displayed strong immunogenicity with potent induction of CD8+ T cells. When combined with anti-Programmed Cell Death Protein 1 (PD-1), the vaccine induced superior tumor clearance and survival in murine tumor models expressing P1A compared with anti-PD-1 alone. Remarkably, ChAdOx1/MVA P1A vaccination promoted CD8+ T-cell infiltration in the tumors, and drove inflammation in the tumor microenvironment, turning 'cold' tumors into 'hot' tumors. Single-cell transcriptomic analysis of the P1A-specific CD8+ T cells revealed an expanded population of stem-like T cells in the spleen after the combination treatment as compared with vaccine alone, and a reduced PD-1 expression in the tumor CD8+ T cells.

Conclusions These findings highlight the synergistic potency of ChAdOx1/MVA MAGE vaccines combined with anti-PD-1 for cancer therapy, and establish the foundation for clinical translation of this approach. A clinical trial of ChadOx1/MVA MAGE-A3/NY-ESO-1 combined with anti-PD-1 will commence shortly.

INTRODUCTION

Recent developments in the field of immunotherapy have brought about unprecedented improvements in patient outcomes for previously difficult to treat advanced cancers. This is best exemplified by immune checkpoint blockade (ICB)—therapies targeting ligand-receptor interactions that negatively regulate effector T-cell function, or so-called immune checkpoints.[1][2] Inhibiting these immune checkpoint pathways with monoclonal antibodies (mAbs) can enhance the priming of anti-tumor T cells and restore their effector activity.[3] Immune checkpoint inhibitors, particularly those targeting PD-1, Programmed Cell Death Ligand 1 (PD-L1), or Cytotoxic T Lymphocyte-associated Antigen 4 (CTLA-4) induce durable tumor regressions and greatly enhance survival in cancer patients.[4–6] However, despite these successes, in most cancer types, the majority of patients fail to respond and do not experience clinical benefit. This is partly due to a lack of pre-existing antitumor CD8+ cytotoxic T lymphocytes (CTLs).[7] Therapeutic cancer vaccines that can generate CTLs against tumor-specific antigens could therefore improve response rates to ICB. Indeed, the concept of combining ICB with therapeutic cancer vaccination has been tested in the clinic, with vaccination targeting the tumor-causing human papillomavirus.[8]

Melanoma antigen gene (MAGE)-type antigens are tumor-specific antigens that have long been the targets of cancer vaccines due to their unique properties.[9] They are non-mutated antigens encoded by cancer-germline genes, whose expression in normal tissues is mostly restricted to male germline cells that are incapable of presenting antigens

to the immune system due to the lack of Human Leukocyte Antigen (HLA) molecules.[9] Being non-mutated, these antigens are shared by many independent tumors and found in a high proportion of human tumors, as opposed to mutated neoantigens. Peptides derived from MAGE-type proteins are presented by HLA molecules to tumor-specific T lymphocytes, and antitumor CD8+ T cells from many different patients with cancer were found to recognize MAGE-type antigens,[10–12] indicating that these antigens are highly immunogenic. Previous attempts to develop MAGE-targeting cancer vaccines however have proven unsuccessful, with candidates failing to demonstrate significant efficacy in large-scale clinical trials.[13 14] These studies used a classical vaccine platform with recombinant MAGE-A3 protein and adjuvant formulations, which preferentially induces antibody and CD4+ T-cell responses rather than the strong CD8+ CTL responses necessary for significant antitumor effect.[15 16]

In contrast to traditional vaccine platforms, recombinant viral vector vaccines have recently been shown to induce potent CD8+ T-cell responses in humans.[17] In particular, heterologous prime-boost vaccines using chimpanzee adenovirus ChAdOx1 and modified vaccinia Ankara (MVA) were shown to generate some of the highest magnitude CD8+ T-cell responses against antigens in the settings of infectious diseases and prostate cancer.[17–19] Head-to-head comparisons of multiple platforms have shown the advantage of adenoviral/MVA prime-boost vaccination schemes for inducing CD8+ T-cell responses against a tumor-associated viral antigen.[20] Though these studies can demonstrate adenoviral/MVA prime-boost vaccination is superior in stimulating peripheral antitumor CTL responses, its effect on the tumor microenvironment (TME) is not well explored. The presence of CD8+ T cells and associated inflammation in tumors is linked to improved prognoses and is vital for a positive clinical response to ICB.[7] T-cell inflamed tumor gene expression signatures are better predictors of response than all other variables.[21 22] An effective therapeutic cancer vaccine should therefore be able to promote CD8+ T-cell infiltration into the tumor and induce inflammation in the TME, turning a 'cold' non-inflamed tumor 'hot'. Thus, cancer vaccines have the potential to work synergistically with ICB to improve their efficacy.

Here, we generated recombinant ChAdOx1 and MVA vectors expressing the prototypical MAGE-type antigens MAGE-A3, NY-ESO-1 or their murine counterpart P1A,[23] which shares strong similarities with human MAGE-type antigens including the pattern of expression.[24] The immunogenicity and anti-tumor efficacy of the ChAdOx1/MVA P1A vaccine with and without checkpoint inhibitors was evaluated in mouse tumor models. We show that the ChAdOx1/MVA P1A vaccine boosts the levels of P1A-specific CD8+ tumor-infiltrating lymphocytes (TILs) in an otherwise poorly infiltrated tumor, and enhances response to anti-PD-1 blockade, resulting in better tumor control and improved survival. Finally, we assessed the immunogenicity of the ChAdOx1/MVA

MAGE-A3-NY-ESO-1 vaccines to support an imminent clinical trial study.

MATERIALS AND METHODS
Mice
Six to eight-week-old female CD1, C57BL/6 and DBA/2 mice used in this study were purchased from Envigo, UK.

Viral vectors
The coding sequence of P1A (NCBI RefSeq NP_035765.1), MAGE-A3 (NCBI RefSeq NM_005362.3) and NY-ESO-1 (GenBank: U87459.1) were purchased as strings DNA fragments from GeneArt (Thermo Fisher Scientific, Paisley, UK). Further details on vector construction are described in the online supplemental materials.

Vaccinations and immune checkpoint inhibitor treatments
Vaccinations were performed at a dose of either 10^8 or 10^7 infectious units of ChAdOx1 virus and 10^7 or 10^6 plaque forming units of MVA virus, given via intramuscular (i.m.) injection in 50 µL total volume. Anti-PD-1 (BioXcell, clone RMP114), anti-CTLA-4 (BioXcell, clone 9H10) or the relevant isotype control (BioXcell, clone 2A3) were administered via intraperitoneal injection at a dose of 100 µg per mouse, given 3 times at a 3-day interval. For therapeutic efficacy studies, tumor-bearing mice were randomized according to tumor size before treatment.

Cell lines, tumor transplantation and measurements
P815 and 15V4T3 cell lines are of DBA/2 origin and express P1A.[25] B16F10 and MC38 cell lines were obtained from ATCC. Cell lines were regularly mycoplasma tested to confirm the absence of infection. To initiate tumor growth, 1×10^6 (15V4T3, P815) or 1×10^5 (B16F10, MC38) tumor cell suspension was implanted subcutaneously (s.c.) in the right flank of the mice. Tumor growth was measured 2–3 times per week and mice were sacrificed when tumor size reached 10 mm or 12 mm in any direction. Tumor volume (V) was calculated according to the formula: $V = ((\text{length (mm)} \times \text{width}^2 \text{ (mm)}) \times 0.52)$. For mean tumor volume calculations, the final end-point value recorded when a mouse was sacrificed was carried forward to enable the calculation of a group mean at later time points.

Surface staining, intracellular cytokine staining and flow cytometry
Peripheral blood mononuclear cells (PBMCs) and bulk splenocytes were harvested as described previously.[26] Tumor masses were surgically excised and weighed. Tumor single cell suspension was obtained by dissociation of tissues using a gentleMACS Dissociator (Miltenyi Biotec) according to the manufacturer's instruction. For surface staining, cells were incubated for 10 min at 4°C with 5 µg/mL anti-CD16/CD32 (clone 2.4G2, BD Biosciences) to block Fc receptors, washed, and then stained for 30 min at 4°C with PE-conjugated

H-2L^d/P1A$_{35-43}$- LPYLGWLVF multimer (manufactured and provided by Ludwig Institute for Cancer Research, Brussels, Belgium). Cells were then washed and stained for 20 min at 4°C with viability dye (LIVE/DEAD Aqua, Invitrogen) and fluorescently conjugated mAbs against surface molecules according to different staining panels; anti-CD3-APC (clone 17A2), anti-CD8-FITC (clone 53–6.7), anti-CD4-AlexaFluor-700 (clone GK1.5), anti-PD-1-PE-Cy7 (clone 29F.1A12), anti-TIM-3-BV421 (clone RMT3-23), anti-LAG-3-BV650 (clone C9B7W), anti-CD11b-FITC (clone M1/70), anti-CD11c-BV650 (clone N418), anti-F4/80-BV421 (clone BM8), anti-Ly6C-APC (clone HK1.4), anti-Ly6G-PE-Cy7 (clone 1A8). For intracellular cytokine staining (ICS), cells were stimulated with 4 µg/mL of MAGE-A3, NY-ESO-1 or P1A 15-mer peptide mix (PepSets Peptide library, Mimotopes) in the presence of DNaseI (20 µg/mL, Roche) and costimulatory anti-CD28 (2 µg/mL, Tonbo Biosciences) at 37°C for 5 hours, adding brefeldin A (10 µg/mL, BioLegend) for the last 4 hours to allow accumulation of intracellular cytokines. Cells were then surface stained, fixed and permeabilized (BD Cytofix/Cytoperm), then stained intracellularly for cytokine production with anti-IFN-γ-APC (clone XMG1.2), anti-IL-2-PE (clone JES6-5H4), and anti-TNF-α-BV650 (clone MP6-XT22), and then acquired on a Fortessa flow cytometer (BD Biosciences). All mAbs were purchased from BioLegend. Data were analyzed with FlowJo software v10 (Tree Star, Ashland, Oregon). Analysis of multifunctional CD8$^+$ T-cell responses was performed via a Boolean analysis of IFN-γ$^+$, TNF-α$^+$, IL-2$^+$ events in the CD8$^+$ gate using FlowJo. Pestle (NIH, Bethesda) and SPICE (Vaccine Research Centre, NIH, Bethesda) software were used to generate graphical representations of proportions of T cells expressing 1, 2 or all 3 cytokines.

RNA sequencing

For bulk RNA sequencing, sample cDNA libraries were prepared following poly-A selection to enrich for mRNA and then sequenced as 150 bp paired-end reads on a NovaSeq 6000 (Illumina). For scRNA-seq, tumors and spleens were processed into single cell suspension. Biological replicates (n=10) for each experimental condition were pooled together at the tissue processing stage. Around 5000 live CD3$^+$CD8$^+$P1A$_{35-43}$-LPYLGWLVF$^+$ cells from each condition were sorted by fluorescence activated cell sorting using a BD FACSAria III (BD Biosciences). Sorted cells from each experimental condition were loaded into a Chromium single-cell sorting system (10× Genomics). Single-cell RNA libraries were prepared using 10× Genomics Chromium platform and reagents according to the manufacturer's instructions by the Oxford Genomics Centre, University of Oxford. Details of sequencing data analysis are described in the online supplemental materials.

Statistical analysis

Statistical analyses were carried out using Prism v8.0 (GraphPad). For immunogenicity study data, to determine significance comparing between multiple groups a Kruskal-Wallis test with a Dunn's post hoc analysis was performed. For comparisons between only two groups a Mann-Whitney U-test was performed. To determine significance between responses at different time-points within the same group a Wilcoxon matched-pairs signed rank tested was performed. For gene expression studies, ordinary one-way analysis of variance (ANOVA) was performed followed by Tukey's post hoc to determine significance between individual groups. Statistically significant differences in tumor growth between different groups was determined by two-way ANOVA followed by Tukey's post hoc test. Survival curves were created using the Kaplan-Meier method and statistical significance between different groups was determined using the log-rank (Mantel-Cox) test. All p values<0.05 were considered statistically significant.

RESULTS

ChAdOx1/MVA P1A prime-boost vaccination induces robust P1A-specific CD8$^+$ T-cell responses

We first evaluated the immunogenicity of the ChAdOx1/MVA vectors encoding the murine MAGE-type antigen P1A, and the effect of the molecular adjuvants, namely the MHC-class II-associated invariant chain transmembrane domain (Ii-TMD) and the tissue plasminogen activator (tPA) signal sequence.[27 28] DBA/2 mice were given a ChAdOx1-P1A (±Ii) prime vaccination and then received an MVA-P1A boost vaccination 4 weeks later (figure 1A). PBMCs from vaccinated mice were stimulated with overlapping P1A peptides and the fraction of cytokine-producing P1A-specific CD8$^+$ T cells assessed by flow cytometry (figure 1B). Following prime vaccination with either ChAdOx1-P1A or ChAdOx1-Ii-P1A, significantly higher frequencies of IFN-γ-producing CD8$^+$ T cells were detected compared with the PBS control group (figure 1C). Notably, fusion of the Ii-TMD sequence to P1A increased the frequencies of P1A-specific CD8$^+$ T cells induced by ChAdOx1 vaccination. Furthermore, the MVA-P1A boost greatly increased the magnitude of the P1A-specific CD8$^+$ T-cell response (figure 1C). No P1A-specific CD4$^+$ T-cell response was observed, in line with the fact that no CD4 epitope has been described for P1A (online supplemental figure S1A). Frequencies of H-2L^d P1A$_{35-43}$LPYLGWLVF$^+$ CD8$^+$ T cells post MVA vaccination were similar to frequencies of IFN-γ$^+$ CD8$^+$ T cells detected by ICS, further confirming induction of a strong P1A-specific CD8$^+$ T-cell response (figure 1D). While more than 50% of the vaccine-induced CD8$^+$ T cells were polyfunctional, producing at least two cytokines among IL-2, TNF-α and IFN-γ, we did not detect any significant differences between different groups (figure 1E). The inclusion of tPA to P1A in the MVA vector did not significantly alter
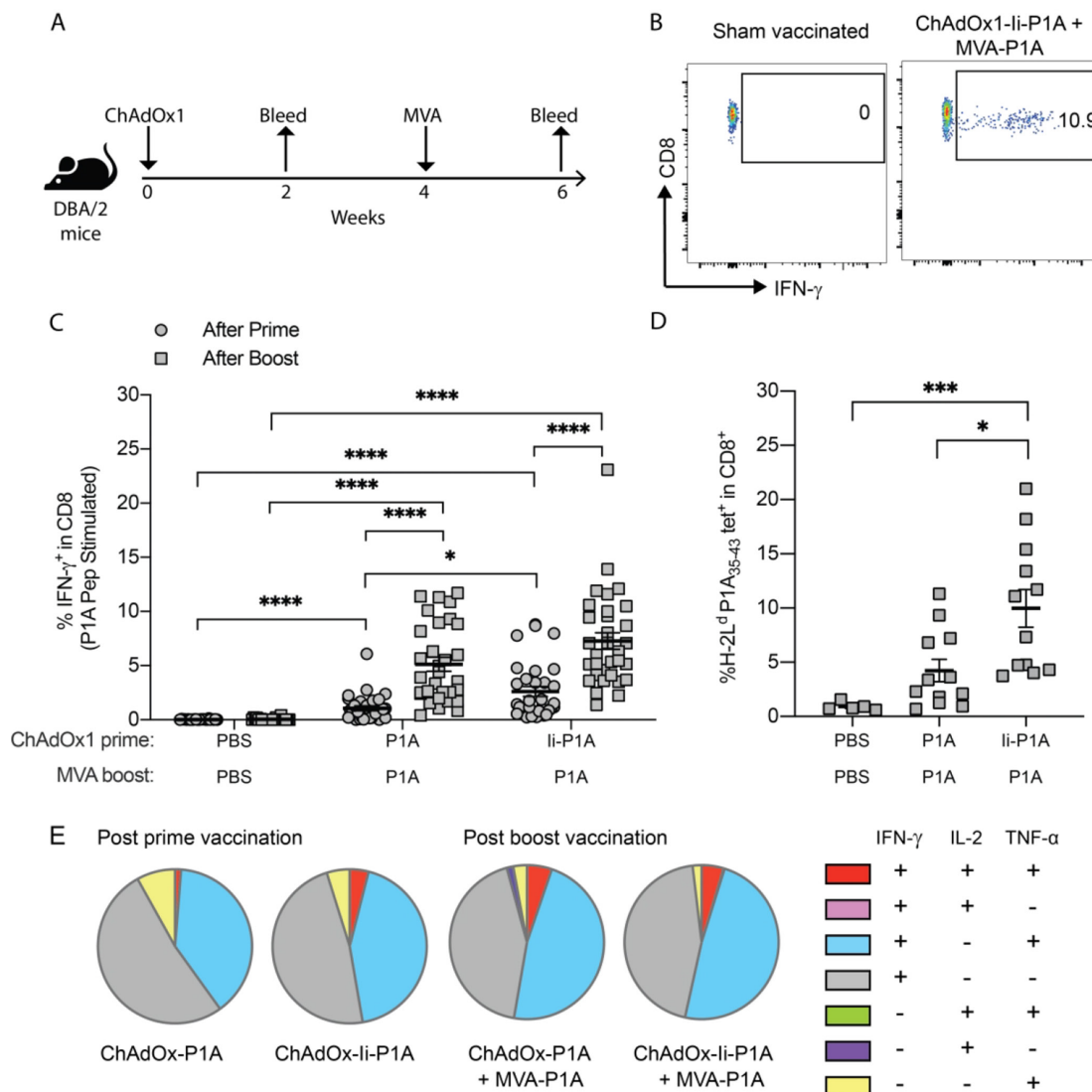
Figure 1 ChAdOx1/MVA P1A vaccination induces robust P1A-specific CD8$^+$ T-cell responses. DBA/2 mice received a prime vaccination via intramuscular (i.m.) injection with 10^8 IU of ChAdOx1-P1A ± Ii or a sham vaccination with PBS then 4 weeks later received a boost vaccination with 10^7 PFU of MVA-P1A. Mice were bled 10–20 days after vaccination with ChAdOx1 and 9–14 days after vaccination with MVA. (A) Experimental scheme. (B) PBMCs were stimulated *ex vivo* with 4 µg/ml of P1A peptide pools and the percentage of cytokine-producing P1A-specific CD8$^+$ T cells in the blood after each vaccination was then determined by intracellular cytokine staining (ICS) and flow cytometry. The representative dot plots show gating of IFN-γ^+ CD8$^+$ T cells. (C, D) Percentages of IFN-γ^+ cells among CD8$^+$ T cells after prime (closed circles) and boost (closed squares) are shown in (C) and percentages of P1A$_{35-43}$ tetramer$^+$ CD8$^+$ T cells after boost are shown in (D). Data are shown as mean ± SEM, each symbol represents an individual mouse with 5–10 mice per group, pooled from 2–4 independent experiments. Statistically significant differences between groups were determined by a Kruskal-Wallis test with Dunn's multiple comparisons test. *, p ≤ 0.05, ***, p ≤ 0.001 ****, p ≤ 0.0001. (E) Cytokine production profile of P1A-specific CD8$^+$ T cells is shown. A Boolean analysis was performed in FlowJo software to calculate the percentage of CD8$^+$ T cells producing only one, a combination of two, or all three of IFN-γ, IL-2 and TNF-α. Pie charts show the mean relative proportion of each cytokine producing subset out of the total antigen-specific CD8$^+$ T cells.

the frequencies of vaccine-induced P1A-specific CD8$^+$ T cells (online supplemental figure S1B).

ChAdOx1/MVA P1A vaccination exhibits good therapeutic efficacy against early established 15V4T3 tumors

The high magnitude P1A-specific CD8$^+$ T-cell responses induced by ChAdOx1/MVA P1A vaccination translated into tumor protection when vaccinated mice were challenged with tumor cells from either P815 or 15V4T3,

two P1A-expressing mastocytoma cell lines[25 29] (online supplemental figure S2A-E). Then, we further tested the vaccine therapeutic efficacy against 15V4T3 tumors, which showed lower rates of spontaneous tumor resolution than P815 (online supplemental figure S2F). Three different ChAdOx1/MVA P1A vaccination doses and schedules, aimed at shortening vaccination time, were tested against early established 15V4T3
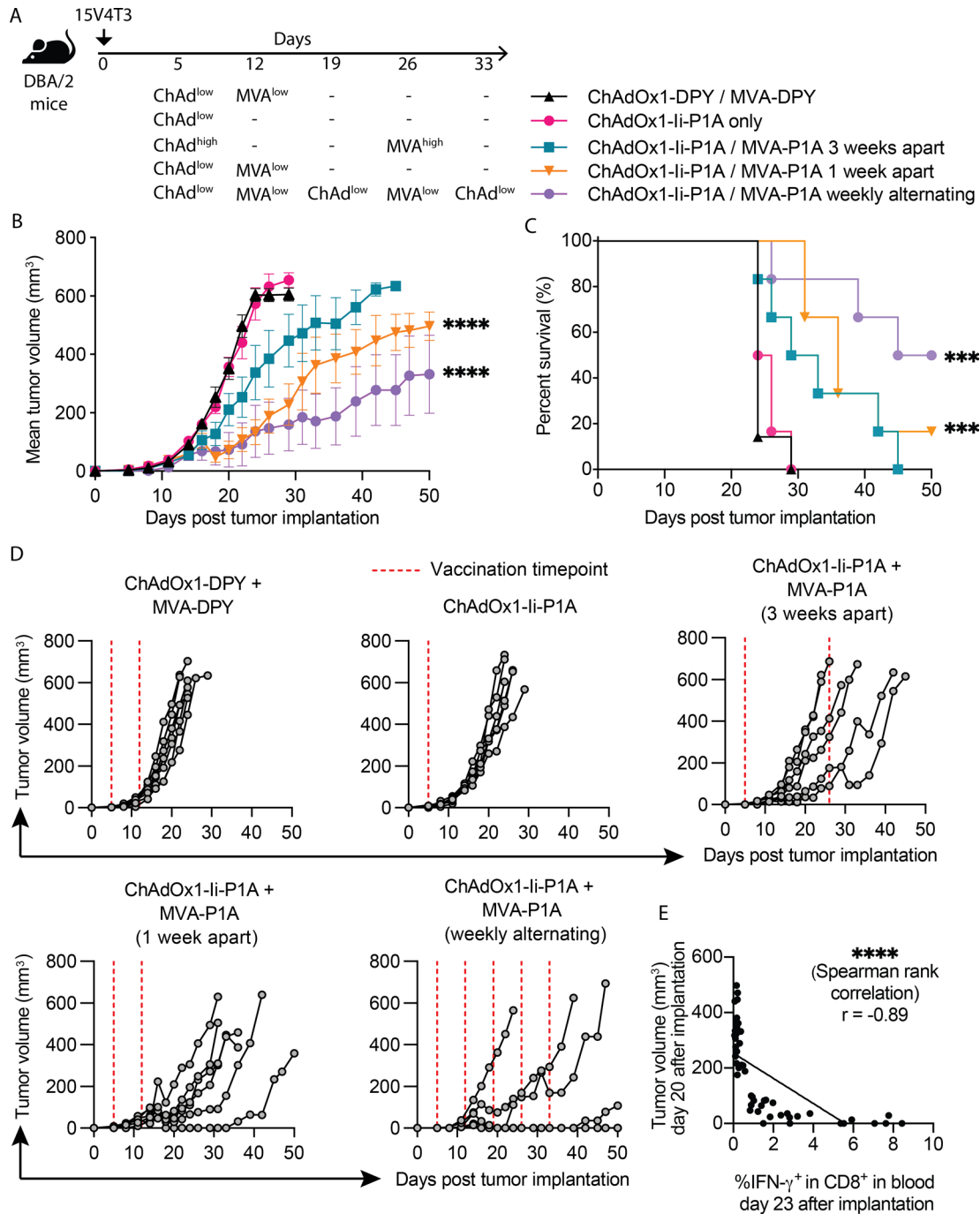
Figure 2 ChAdOx1/MVA P1A vaccination exhibits good therapeutic efficacy against early established 15V4T3 tumors. (A) DBA/2 mice were implanted with 1×10^6 15V4T3 cells via subcutaneous (s.c.) injection. Five days after tumor implantation, mice were vaccinated with ChAdOx1-Ii-P1A and MVA-P1A according to the schedules shown and indicated doses of virus: ChAd^{high} - 10^8 IU, ChAd^{low} - 10^7 IU, MVA^{high} - 10^7 PFU and MVA^{low} - 10^6 PFU. Tumor growth was followed for 50 days and mice culled when tumors reached 12 mm in any direction. (B-D) Mean tumor growth (B), survival (C) and individual tumor growth (D) for each group are shown. (E) Tumor size on day 20 post implantation was correlated with the frequency of blood IFN-γ^+ CD8$^+$ T cells detected by ex vivo P1A peptide stimulation and ICS on day 23. Tumor growth data are presented as mean tumor volume (mm^3) ± SEM. Each group contained 6-7 mice, with data representative of 2 independent experiments. Statistically significant differences between groups were determined by a two-way ANOVA with Tukey's post hoc test for tumor volume data and a log-rank test for survival data. Statistical differences are shown only between vaccinated groups and ChAdOx/MVA control group. Significance of correlation was determined through a Spearman rank test. ***, $p \leq 0.001$ ****, $p \leq 0.0001$.

tumors (5 days after implantation), with a control group receiving ChAdOx1/MVA expressing irrelevant protein DPY (figure 2A). Compared with the control group, mice receiving ChAdOx1/MVA P1A vaccinations showed improved control of 15V4T3 tumor growth (figure 2B,D). Mice in the control group had

mostly succumbed to tumor burden within 24 days post tumor implantation. Conversely mice receiving low-dose ChAdOx1/MVA P1A vaccinations, either given 1 week apart or weekly alternating vaccinations, had significantly improved tumor control and longer survival (figure 2B–D). This was most apparent in the groups receiving weekly alternating vaccinations. This result is in line with a previous study showing that low dose weekly alternating ChAdOx1/MVA vaccinations provided superior control of tumor growth in prostate cancer models.[30] A single log-fold reduced dose of ChAdOx1-Ii-P1A did not demonstrate a therapeutic effect, suggesting the MVA boost to be critical for vaccine therapeutic efficacy. P1A-specific T-cell responses in the blood of tumor-bearing mice were assessed as previously by P1A peptide-stimulation and ICS of PBMCs. Interestingly, a strong negative correlation (Spearman rank, r=−0.89) was observed between tumor burden and frequencies of peripheral IFN-γ-producing CD8$^+$ T cells, suggesting that the vaccine-induced response was likely responsible for tumor control (figure 2E).

ChAdOx1/MVA P1A vaccination combined with ICB enhances tumor control

Though vaccination alone was able to control early established tumors, the majority of cancers are diagnosed at a late stage. Also, we observed PD-L1 to be constitutively expressed on the surface of 15V4T3 cells, and its expression further upregulated by IFN-γ stimulation (online supplemental figure S3A–D). Therefore, we tested the combination of vaccination with ICB against more established 15V4T3 tumors (figure 3A). Initiating vaccination at a later time-point against more established tumors (day 8 compared with day 5 in previous therapeutic experiments, figure 2) greatly reduced the therapeutic effect of ChAdOx1-Ii-P1A/MVA-P1A vaccination alone (figure 3B–D). Compared with the PBS control group, there was no significant control of tumor growth (figure 3B) and only a slight improvement in survival was observed (figure 3C). Interestingly, ICB monotherapy with either anti-PD-1 or anti-CTLA-4 alone was similarly ineffective at controlling tumor growth. Anti-PD-1 alone only delayed tumor growth (figure 3B) and increased survival by a small amount (figure 3C) compared with the PBS control. However, the combination of ChAdOx1-Ii-P1A/MVA-P1A vaccination with either anti-PD-1 or anti-CTLA-4 strongly improved tumor control over any modality given alone. Tumor growth was significantly reduced in the ChAdOx1-Ii-P1A/MVA-P1A+anti-PD-1 combination group compared with both ChAdOx1-Ii-P1A/MVA-P1A only and anti-PD-1 only groups (figure 3B), and survival was significantly improved (figure 3C). Indeed, half of the mice in the ChAdOx1-Ii-P1A/MVA-P1A+anti-PD-1 group were able to completely resolve their tumors and were still alive after 50 days (figure 3D; n=3/6). Though the combination of vaccination with anti-CTLA-4 resulted in better control of tumor growth over

the respective single treatment groups, survival was not significantly increased. Further still, the combination of ChAdOx1-Ii-P1A/MVA-P1A vaccination with anti-PD-1 was more efficacious than with anti-CTLA-4; over the course of 50 days the mean tumor growth in the ChAdOx1-Ii-P1A/MVA-P1A+anti-PD-1 group was significantly less than the ChAdOx1-Ii-P1A/MVA-P1A+anti-CTLA-4 group (figure 3B). These results suggested that there was particular synergy in the combination of ChAdOx1/MVA P1A vaccination with anti-PD-1 blockade for generating a potent antitumor effect.

ChAdOx1/MVA P1A vaccination promotes CD8$^+$ T-cell infiltration and drives inflammation in the TME

We then sought to determine the effect of ChAdOx1/MVA P1A vaccination ±anti-PD-1 treatment on T-cell infiltration and inflammation in the 15V4T3 TME. First, the T-cell infiltration of 15V4T3 tumors was compared with well-defined tumor models—MC38, a 'hot' relatively T-cell inflamed and ICB responsive tumor and B16F10, a 'cold' poorly immunogenic and ICB unresponsive tumor.[31] 15V4T3 tumors were poorly infiltrated by CD8$^+$ T cells, containing on average significantly fewer TILs than MC38 tumors, and slightly fewer than even B16F10 tumors (online supplemental figure S3E,F). This extreme paucity of CD8$^+$ TILs in 15V4T3 suggests it is more akin to an immune 'cold' tumor, and this could likely underlie the low effect of anti-PD-1 treatment given as monotherapy. Next, 15V4T3 tumors were harvested from mice following vaccine ±anti-PD-1 treatment at 20 days after implantation, and the immune composition was profiled by flow cytometry (figure 4A). Tumors from mice receiving either vaccine alone or vaccine +anti-PD-1 contained significantly higher percentages and total numbers of CD8$^+$ TILs compared with the PBS control and anti-PD-1 only groups (figure 4B–D). Conversely, anti-PD-1 treatment alone had no effect on CD8$^+$ T-cell infiltration into the tumor compared with PBS control mice, and tumors from vaccine +anti-PD-1 treated mice did not have more T cells than those receiving vaccine alone (figure 4B–D). Analysis of the P1A-specific CD8$^+$ TILs by tetramer staining showed that ChAdOx1/MVA P1A vaccination significantly increased both the percentage and total number of P1A$_{35-43}$ tetramer$^+$ cells in the TME (figure 4E–G). In numerical terms, this represented at least a 10-fold increase in numbers of P1A$_{35-43}$ tetramer$^+$ CD8$^+$ T cells in the tumor. We also analyzed tumor infiltration of both CD11b$^+$ Ly6C^{+hi} Lyg6G$^-$ and CD11b$^+$ Ly6C^{+int} Ly6G$^+$ cells, corresponding to monocytic myeloid-derived suppressor cell-like and granulocytic myeloid-derived suppressor cell-like phenotype, respectively,[32] but no significant difference was observed between different treatment groups (online supplemental figure S4).

Gene expression profiles (GEPs) in the 15V4T3 tumors following treatment were further assessed at the transcriptional level using RNA sequencing.
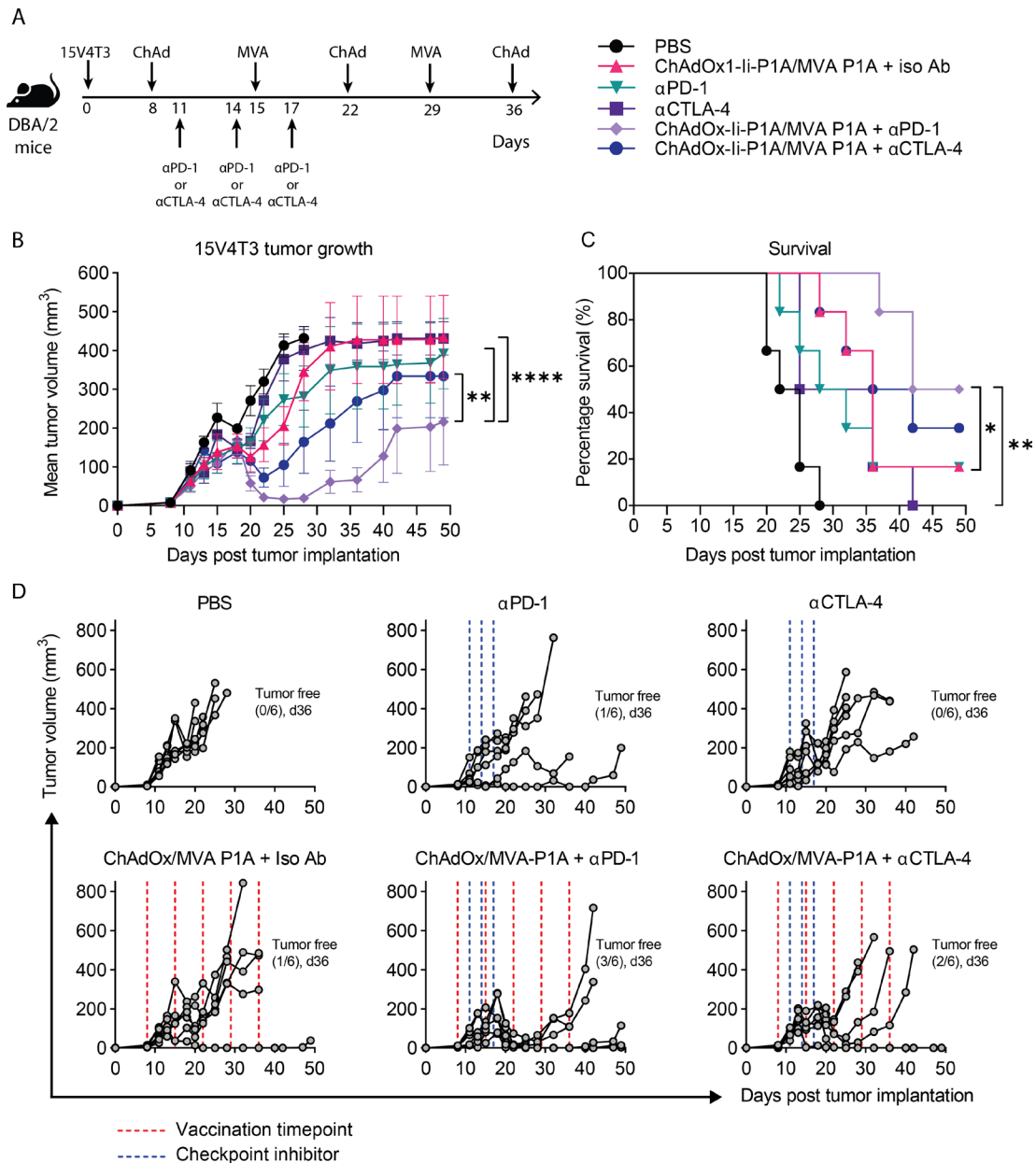
Figure 3 ChAdOx1/MVA P1A vaccination combined with immune checkpoint blockade enhances tumor control. (A) DBA/2 mice were implanted with 1×10^6 15V4T3 cells via s.c. injection. Eight days after tumor implantation, mice were randomized into experimental groupings according to tumor volume. Starting on day 8, mice then received vaccinations of 10^7 IU ChAdOx1-li-P1A / 10^6 PFU MVA-P1A alternating weekly or a PBS sham, and were treated with 3-doses of 100 µg anti-PD-1, anti-CTLA-4 or an isotype control antibody according to the schedule as shown. Tumor growth was followed for 50 days and mice were culled when tumor size reached size endpoints. (B-D) Mean tumor growth (B), survival curves (C) and individual tumor growth kinetics (D) for each group are shown. Tumor growth data in (B) are presented as mean tumor volume (mm^3) ± SEM. Each group contained 6 mice, with data representative of 2 independent experiments. Statistically significant differences in tumor volume between groups were determined by a two-way ANOVA followed by Tukey's post hoc test and statistical differences in survival data were determined by a log-rank test. *, $p \le 0.05$, **, $p \le 0.01$ ****, $p \le 0.0001$.

Differentially expressed genes (DEGs) were determined for each treatment group compared with the PBS control (online supplemental figure S5A), demonstrating that ChAdOx1/MVA P1A vaccination, either alone or combined with anti-PD-1, had a dramatic effect on tumor gene expression patterns (online supplemental figure S5B). Tumors from vaccinated mice had starkly different GEPs than those from groups not receiving vaccination (online supplemental figure S5C). Gene expression signatures associated with T-cell inflammation and IFN-γ response, which were shown to be predictive of clinical response to anti-PD-1 treatment,[21][33] were upregulated in the tumors of vaccinated mice (figure 4H). All samples from vaccinated mice had higher T-cell inflammation and IFN-γ response gene expression signature scores than unvaccinated
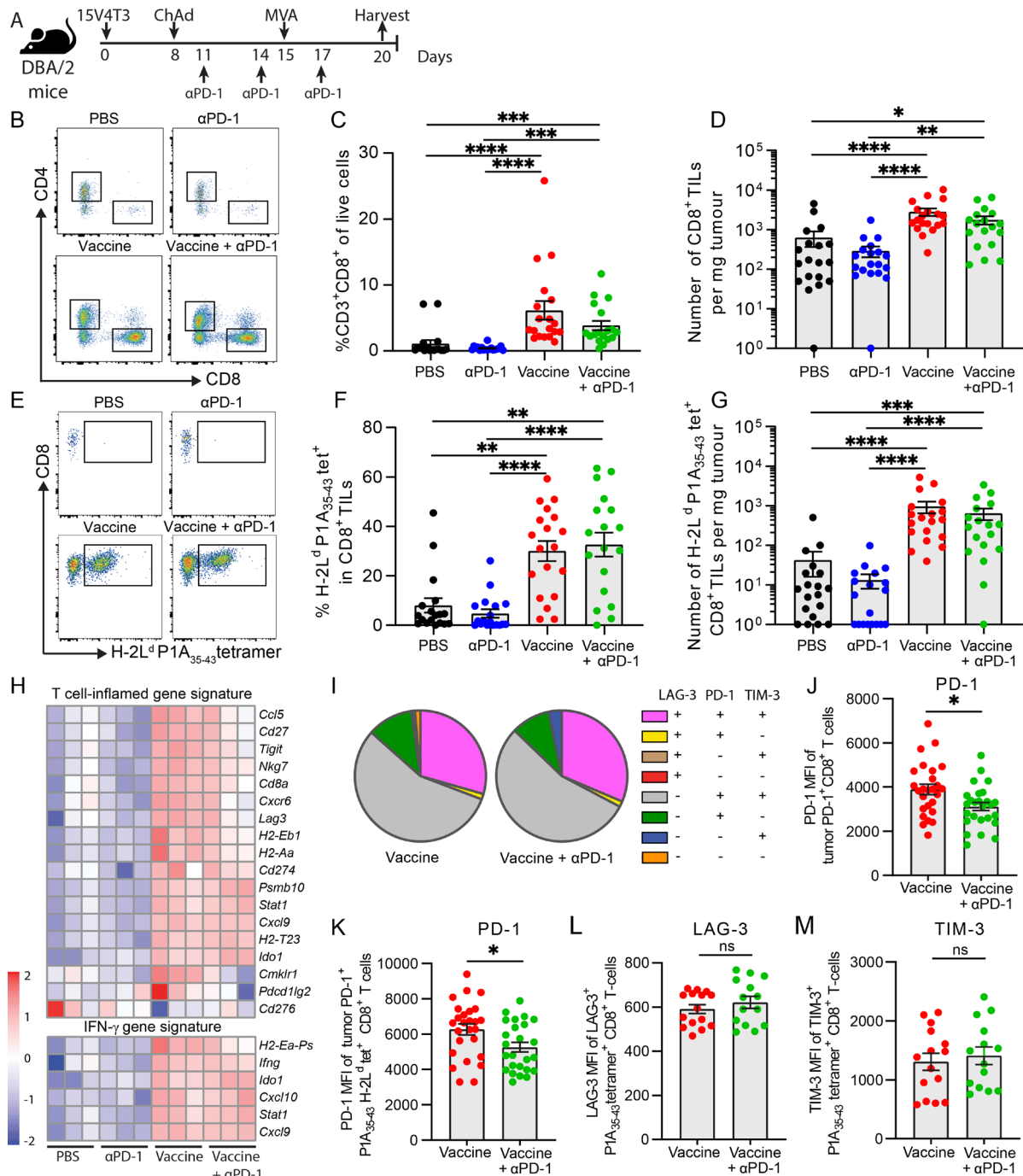
Figure 4 ChAdOx1/MVA P1A vaccination promotes CD8+ T-cell infiltration into the TME. (A) DBA/2 mice were implanted with 1×10^6 15V4T3 cells via s.c. injection and treated with PBS control, ChAdOx-Ii-P1A (10^7 IU) /MVA-P1A (10^6 PFU), anti-PD-1 or combination treatment. Mice were sacrificed following treatment, and tumors surgically excised for analysis of immune cell infiltrate by flow cytometry. (B) Representative flow cytometry gating plots of CD8+ TILs. (C) Percentage and (D) total numbers of CD8+ TILs in 15V4T3 tumors, as quantified by flow cytometry. (E) Representative flow cytometry gating plots of P1A$_{35-43}$ tet+ CD8+ TILs. (F) Percentage and (G) total numbers of P1A$_{35-43}$ tet+ CD8+ TILs in 15V4T3 tumors, as quantified by flow cytometry. (H) RNA-sequencing analysis of tumor mRNA from 3 mice per group. Heatmaps showing log-CPM expression values of T-cell inflamed and IFN-γ gene expression signatures across all samples. Gene expression level has been scaled by Z-score, indicated by the heatmap color key. (I) Expression of PD-1, LAG-3 and TIM-3 receptors on tumor CD8+ T cells from vaccine ± anti-PD-1 groups was evaluated by flow cytometry. Pie charts show the mean relative proportion of P1A-specific CD8+ T cells expressing combinations of the receptors. (J) PD-1 mean fluorescence intensity (MFI) of tumor PD-1+ CD8+ TILs. (K) PD-1 MFI of PD-1+ P1A$_{35-43}$ tet+ CD8+ TILs (L) LAG-3 MFI of LAG-3+ P1A$_{35-43}$ tet+ CD8+ TILs. (M) TIM-3 MFI of TIM-3+ P1A$_{35-43}$ tet+ CD8+ TILs. Tumor immune cell infiltrate data are shown as mean ± SEM. Each symbol represents an individual mouse, with 7-10 mice per group, pooled from 2-3 independent experiments. Statistically significant differences between multiple groups were determined by a Kruskal-Wallis test with Dunn's multiple comparisons test, between only two groups with a Mann-Whitney U test. *, p ≤ 0.05, **, p ≤ 0.01, ***, p ≤ 0.001, ****, p ≤ 0.0001.

mice (online supplemental figure S5D). Gene set variation analysis further confirmed tumors from vaccinated mice to be strongly enriched for expression of other previously established inflammatory and T-cell response gene sets (online supplemental figure S5E). In contrast to this, anti-PD-1 monotherapy had an insignificant effect on gene expression in the tumor, with no statistically significant DEGs identified (online supplemental figure S5A–C). Overexpression of proinflammatory factors *Ifng*, *Cxcl9*, *Cxcl10*, *Ccl3*, *Ccl5* and *Xcl1* in the tumors of vaccinated mice was further confirmed by RT-qPCR in a larger cohort of mice (online supplemental figure S6A), and by immunohistochemical staining for CCL5 and CXCL9, along with CD8 (online supplemental figure S6B).

We then further analyzed tumor-infiltrating CD8+ T-cell phenotype by flow cytometry for expression of the negative immune checkpoint receptors PD-1, LAG-3 and TIM-3. High expression of these receptors was observed on tumor P1A-specific CD8+ T cells, with the majority being PD-1+ TIM-3+ double positive, and a large fraction being PD-1+ TIM-3+ LAG-3+ triple positive (figure 4I). We did not, however, detect much difference in the proportion between the two vaccinated groups. Interestingly, a reduction in the surface expression level of PD-1 on CD8+ and P1A-specific CD8+ TILs was observed in the tumors of the vaccine + anti-PD-1 combination group (figure 4J,K), but surface expression levels of LAG-3 and TIM-3 were not different (figure 4L,M). As PD-1 expression is also an indication of T-cell activation, it is hard to conclude that T cells from the combination group are less exhausted with less PD-1 expression. However, we found that almost 100% of P1A-specific CD8+ T cells in the tumors in both groups express PD-1, indicating these are all activated T cells, and the ones with lower PD-1 expression in the combination group may have an advantage to overcome the negative PD-L1/PD-1 signaling in the TME,[34] especially given that 15V4T3 tumor cells expressed high levels of PD-L1 (online supplemental figure S3A–C).

Single-cell transcriptomic analysis of P1A-specific CD8+ T cells identifies stem-like and effector gene signatures in the spleen and tumor

Next, we further characterized the vaccine-induced P1A$_{35-43}$-specific CD8+ T cells from 15V4T3 tumor-bearing mice by single-cell RNA-sequencing (scRNA-seq) analysis. P1A$_{35-43}$ tetramer+ cells from the spleens and tumors of mice receiving vaccine alone (referred to as spleen_vac and tumor_vac, respectively) and those receiving both vaccine and anti-PD-1 treatment (referred to as spleen_combi and tumor_combi, respectively) (figure 5A) were analyzed. Mice receiving anti-PD-1 only did not have P1A-specific CD8+ T cells in sufficient numbers for analysis. Unsupervised clustering of single cells segregated cells into eight distinct clusters based on GEPs and were visualized by uniform manifold approximation and projection (UMAP), which broadly recapitulated two major cell states (figure 5B). Clusters 1

and 4 were referred to as 'stem-like' CD8+ T-cell clusters as they primarily contained cells with upregulation of genes known to characterize a stem-like state such as *Tcf7*, *Sell* and *Lef1* (figure 5C and online supplemental figure S7). In contrast, clusters 0, 2, 3, 5, 6, and 7 were defined as 'effector' CD8+ T-cell clusters, as they primarily contained cells with upregulation of genes encoding functional effector molecules such as *Gzmb* and *Ifng*, and those encoding inhibitory receptors such as *Tigit* and *Pdcd1* that are characteristic of highly activated but also potentially exhausted CD8+ T cells (figure 5C and online supplemental figure S7).[35] K-nearest neighbor clustering data showed that the segregation of cells into different clusters was more strongly influenced by tissue of origin than anti-PD-1 treatment status (figure 5D). Major tissue-dependent differences were observed in terms of cluster proportion, with spleen having more stem-like cells than the tumor, while the majority of the tumor P1A-specific CD8+ T cells were effector cells (figure 5E). Interestingly, we also observed spleen_combi to have a higher proportion of cells in the stem-like clusters compared with spleen_vac, whereas no noticeable difference in cluster composition was detected between tumor_combi and tumor_vac (figure 5E).

To further characterize the differentiation states of single cells from each condition, we constructed gene signatures that characterize each tissue/treatment setting using the DEGs between spleen_combi and spleen_vac, as well as those between tumor_combi and tumor_vac (online supplemental table S2), and measured their expression scores in each cell. Hierarchical clustering correlation analysis with stem-like and exhaustion T-cell signatures from other recent studies[36–41] (online supplemental table S3) showed an interesting association pattern. Gene signatures that were upregulated when comparing combination to vaccine treatment (SpleenCombi_vs_SpleenVac_UP and TumorCombi_vs_TumorVac_UP) were positively correlated with memory and stem-like T cell signatures associated with better ICB response,[36–39] while negatively correlated with exhausted and terminally differentiated T-cell signatures (figure 5F). On the other hand, the gene signatures upregulated in the vaccination-only group when comparing to the combination group (SpleenVac_vs_SpleenCombi_UP and TumorVac_vs_TumorCombi_UP) showed an opposite trend (figure 5F). In line with this observation, comparisons of characteristic stem-like and exhaustion markers between the two treatment groups showed a trend toward higher expression of stem-like markers in cells from spleen_combi than those from spleen_vac (figure 5G). Cells from tumor_combi exhibited a trend toward lower expression of most exhaustion markers compared with those from tumor_vac, despite the absence of a clear trend for the stem-like markers expressed between these two groups (figure 5G). Overall, these observations suggested that the combination of vaccination and anti-PD-1 treatment expanded the population of spleen P1A-specific stem-like CD8+ T cells. As stem-like CD8+ T cells represent the source of T cells that proliferate on PD-1 blockade,[42] this increased stem-like population of
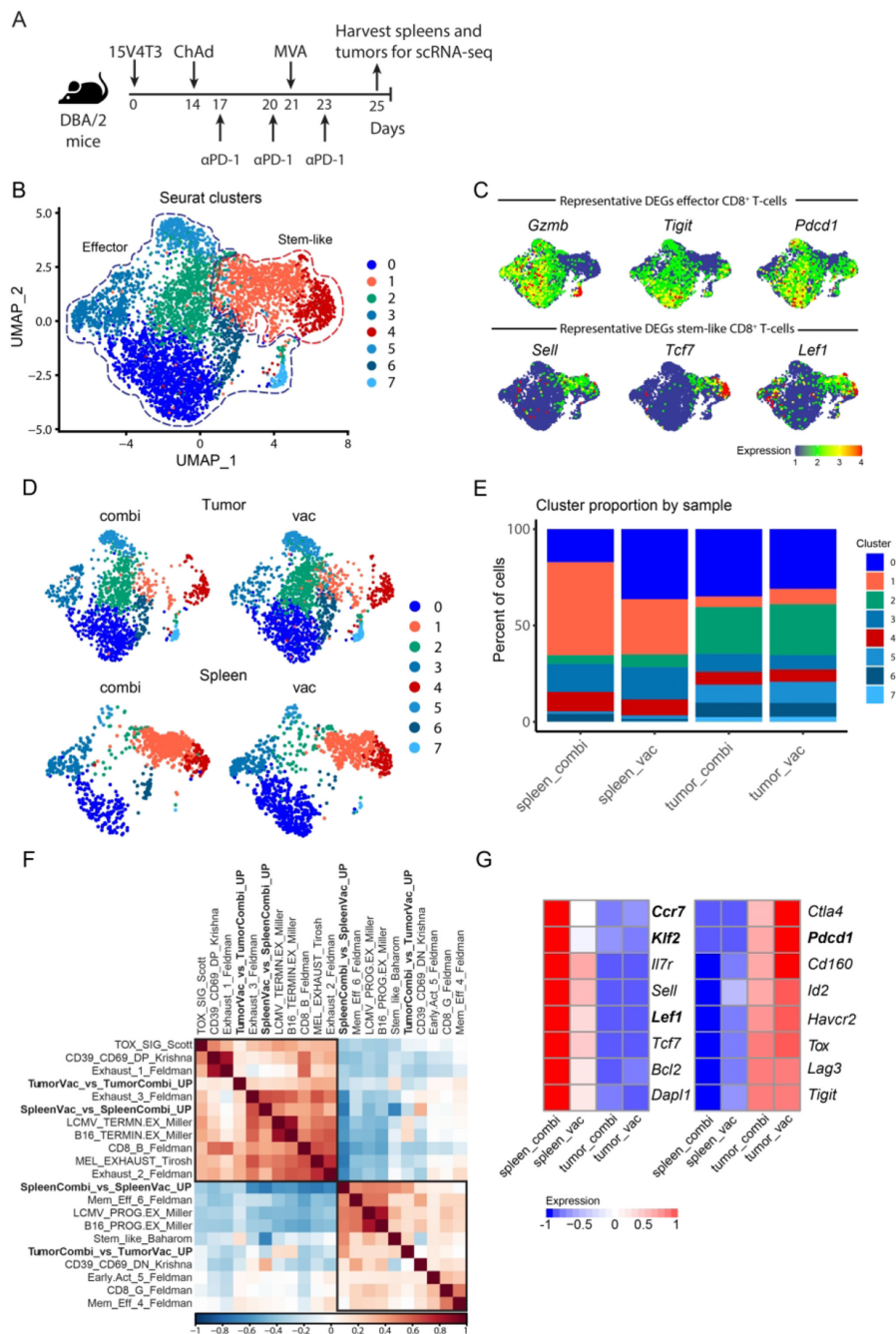
Figure 5 scRNA-seq analysis of P1A-specific CD8^{+} T cells identifies stem-like and effector gene signatures in the spleen and tumor. (A) 15V4T3 tumor-bearing DBA/2 mice were vaccinated with ChAdOx1-Ii-P1A/MVA P1A ± anti-PD-1 treatment (n=10 per group). Tumors and spleens were collected on day 25 and P1A$_{35-43}$-specific CD8^{+} T cells were isolated via H-2L[d] P1A$_{35-43}$ tetramer staining and FACS. The transcriptional profile of P1A$_{35-43}$-specific CD8^{+} T cells was determined via scRNA-seq using a 10X Genomics pipeline. (B) UMAP of P1A$_{35-43}$-specific CD8^{+} T cells sorted from spleens and tumors, separated into eight clusters by k-nearest neighbor clustering analysis using Seurat. (C) UMAPs overlaid with representative DEGs in the effector (top) and stem-like clusters (bottom). (D) P1A$_{35-43}$-specific CD8^{+} T cells cluster in distinct regions of the UMAP space based on their tissue of origin (tumor versus spleen) and treatment strategy (vaccination only versus vaccination combined with anti-PD-1 treatment). (E) Percentage of the eight Seurat clusters represented by each tissue type and treatment. (F) Clustered correlation matrix of exhausted and stem-like gene signatures from previously published data with those identified in combi- and vac-treated P1A$_{35-43}$-specific CD8^{+} T cells from the spleen and tumor (TumorVac_vs_TumorCombi_UP, SpleenVac_vs_SpleenCombi_UP, SpleenCombi_vs_SpleenVac_UP, and TumorCombi_vs_TumorVac_UP). (G) Heatmap showing expression of characteristic stem-like (left) and exhaustion-related (right) genes by P1A-specific CD8^{+} T cells in the spleen and tumor compared between vac and combi groups. Significantly differentially expressed genes are highlighted in bold for comparing spleen_combi vs spleen_vac (left panel) and tumor_combi vs tumor_vac (right panel), as determined with a Wilcoxon rank-sum test with Bonferroni correction. Color key indicates the z-scores of log-normalized expression.
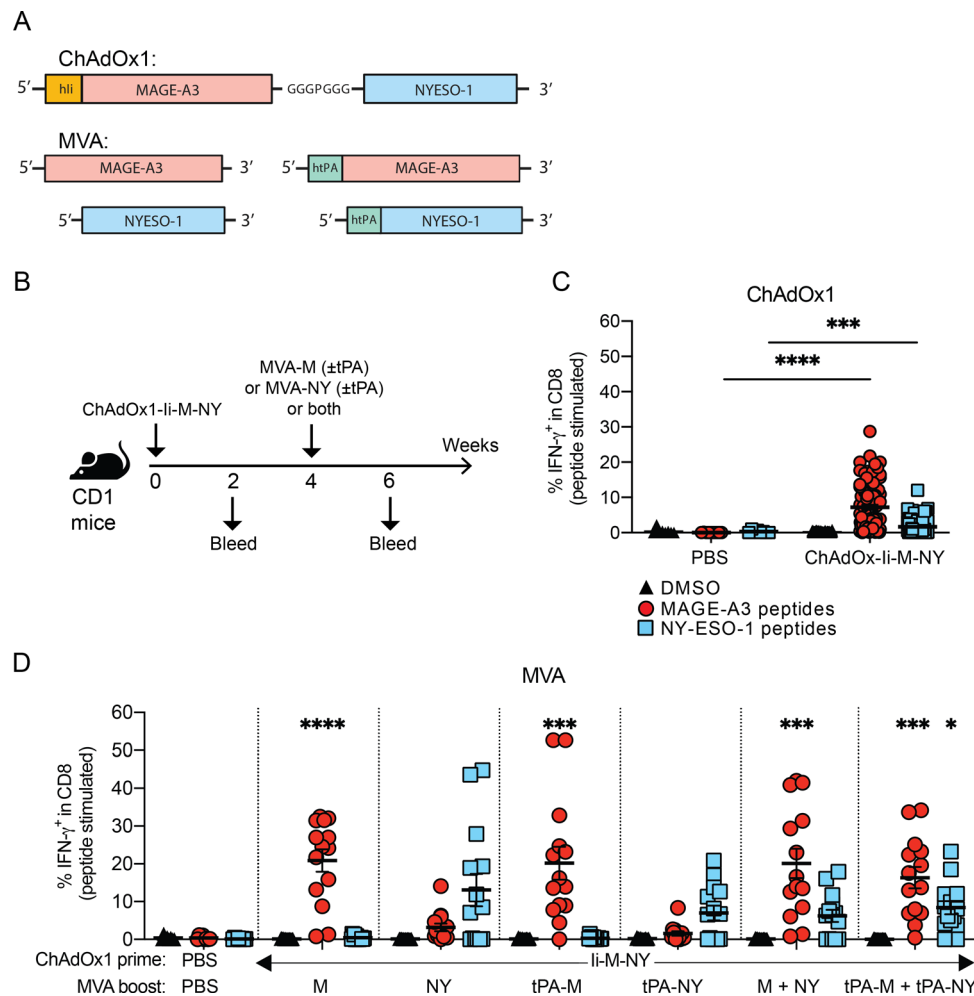
Figure 6 Evaluation of ChAdOx1/MVA prime-boost vaccination targeting MAGE-A3 and NY-ESO-1. (A) Design of ChAdOx1 and MVA vectors encoding the human MAGE-type antigens MAGE-A3 and NY-ESO-1. (B) CD1 outbred mice were vaccinated via i.m. injection according to the schedule shown. Mice received a prime vaccination with 10^8 IU of ChAdOx1-Ii-M-NY. Four weeks after ChAdOx1-M-NY, mice received a boost vaccination via a single injection with 10^7 PFU of either MVA-M (± tPA) or MVA-NY (± tPA), or two injections – one with 10^7 PFU of MVA-M (± tPA) and the other 10^7 PFU of MVA-NY (± tPA). To test the response to vaccination, mice were bled 16 days after ChAdOx1 and 14 days after MVA vaccinations. (C-D) Percentage of IFN-γ^+ CD8$^+$ T cells in the blood after (C) prime vaccination, (D) and the MVA boost vaccinations. PBMCs were stimulated ex vivo with 4 µg/ml of MAGE-A3 or NY-ESO-1 peptide pools, or a DMSO vehicle control. The percentage of antigen-specific IFN-γ^+ -producing CD8$^+$ T cells in the blood after each vaccination was determined by ICS and flow cytometry in response to stimulation with DMSO (black triangles), MAGE-A3 peptides (red circles) or NY-ESO-1 peptides (blue squares). Data are shown as the mean ± SEM and each symbol represents an individual mouse, with 8 mice in the PBS group and 14 mice per ChAdOx1/MVA vaccinated group, pooled from 2 independent experiments. Statistically significant difference is shown compared to the PBS control group and was determined by a Kruskal-Wallis test with Dunn's multiple comparisons test. *, $p \leq 0.05$, **, $p \leq 0.01$ ***, $p \leq 0.001$, ****, $p \leq 0.0001$.

tumor-specific CD8$^+$ T cells could contribute to explain the synergy between vaccine and anti-PD-1 for tumor control.

Evaluation of ChAdOx1/MVA prime-boost vaccination targeting MAGE-A3 and NY-ESO-1 for translation to the clinical setting

The therapeutic efficacy of ChAdOx1/MVA P1A vaccination in combination with anti-PD-1 against P1A-expressing tumors in mice suggests that ChAdOx1/MVA vaccination encoding MAGE-type antigens in combination with ICB has strong potential for translation to the clinic. Therefore, we developed ChAdOx1 and MVA vectors encoding the human MAGE-type antigens

MAGE-A3 (M) and NY-ESO-1 (NY) (figure 6A). A dual-antigen fusion construct was inserted into the ChAdOx1 vector, with the two antigen coding sequences separated by a short polypeptide linker (GGGPGGG), and the TMB domain of human Ii fused to the N-terminus of MAGE-A3. MVA vectors were produced encoding only a single antigen, either MAGE-A3 or NY-ESO-1, with or without human tPA leader sequence (figure 6A). The immunogenicity of these vaccines was investigated using outbred CD1 mice (figure 6B). ChAdOx1-Ii-M-NY vaccination induced a significant increase of IFN-γ^+ CD8$^+$ T cells against both MAGE-A3 and NY-ESO-1 after prime

vaccination (figure 6C), and these CD8 responses further increased after an MVA boost (figure 6D). Mice given a boost vaccination with MVA-M had increased frequencies of MAGE-A3-specific CD8+ T cells, while mice vaccinated with MVA-NY had increased frequencies of NY-ESO-1-specific CD8+ T cells. Equally, vaccination with both MVA vectors (MVA-M and MVA-NY) simultaneously boosted the magnitude against both antigens. Again, inclusion of the tPA signal sequence via fusion to the N-terminus of the recombinant antigen encoded in the MVA vector was not found to significantly alter the magnitude of the antigen-specific CD8+ T-cell response.

DISCUSSION

Positive clinical responses to ICB are limited to a minority of patients as most tumors are not sufficiently immunogenic to spontaneously prime antitumor CTLs.[1] Therapeutic cancer vaccines that induce de novo MAGE-type antigen-specific CTLs could improve ICB response rates in patients with MAGE+ tumors. As compared with neoantigens, MAGE-type antigens are likely less immunogenic, so it is crucial to use a vaccine platform that can induce a strong CD8 response. Here, we evaluated the viral vector ChAdOx1/MVA vaccination regimen in the murine setting using the tumor antigen P1A, the best-known murine equivalent of human MAGE-type antigens. Our results indicate that ChAdOx1/MVA P1A vaccination induces a high magnitude multifunctional P1A-specific CD8+ T-cell response in DBA/2 mice, which has not been observed in previous studies when P1A was delivered in other vaccine platforms,[43] except using arenavirus vector.[44] The induced CD8 response is also comparable to those against other tumor antigens delivered by ChAdOx1/MVA vaccination.[30] The magnitude of the CD8 response can be further enhanced by tethering the Ii-TMD sequence to the N-terminus of P1A encoded in ChAdOx1, corroborating earlier findings showing benefits of linking the transgene to Ii in adenoviral vectors.[27]

It has recently become clear that a CD8+ T cell-inflamed or 'hot' TME underlies a positive clinical response to ICB.[7 22] Tumors obtained after implantation of 15V4T3 cells appear as 'cold' tumors that are largely devoid of CD8+ T cells. However, ChAdOx1/MVA P1A vaccination, either alone or in combination with anti-PD-1 dramatically increased the density of CD8+ T-cells and number of P1A-specific CD8+ T cells in the TME. Although ChAdOx1/MVA vaccination was reported to induce strong antigen-specific CD8+ T-cell responses,[30] its effect on tumor immune infiltration had not been studied. Our results demonstrate that ChAdOx1/MVA P1A vaccination enhances CD8+ T cells levels in poorly infiltrated tumors, and improves response to anti-PD-1 treatment. Vaccination also induces characteristic gene expression signatures of T-cell inflammation and IFN-γ-response, which are the strongest predictors of positive response to anti-PD-1 blockade

in clinical studies.[21 33] Genes that were overexpressed in tumors from vaccinated mice included IFN-γ inducible T-cell chemokines such as *Cxcl9* and *Cxcl10*, which are key mediators regulating CD8+ T-cell recruitment in tumors.[45–47] Increased chemokine expression suggests that ChAdOx1/MVA vaccination generates conditions in the tumor that drive CD8+ T-cell recruitment and inflammation.

When combined with anti-PD-1, the vaccine showed a drastically improved therapeutic efficacy. Tumors from mice receiving the combination did not show increased numbers of vaccine-induced infiltrating CD8+ T cells, but these cells expressed less PD-1 at their surface, suggesting they might be less exhausted, even though they expressed similar levels of LAG-3 and TIM-3. scRNA-seq analysis of P1A$_{35-43}$-specific CD8+ T cells revealed important differences with regard to stem-like vaccine-induced CD8+ T cells, whose proportion was higher in the spleen of mice receiving the combination as compared with vaccine alone. Stem-like CD8+ T cells have been described as a reservoir of less-differentiated CD8+ T cells without effector function but with proliferative potential, which can differentiate into mature effector cells.[48] They are usually located in secondary lymph nodes or tertiary lymphoid structures.[48 49] Stem-like CD8+ T cells mostly develop on chronic antigenic stimulation, and represent a self-renewed source of effector CD8+ T cells, which can populate non-lymphoid tissues, including tumors.[42] Their transition into effector CD8+ T cells is stimulated by PD-1 blockade, and as such they provide the proliferative burst of CD8+ T cells that is observed during anti-PD-1 therapy and mediates tumor rejection.[42 50] It is possible that the better antitumor efficacy we observed with the combination treatment results from this increased stem-like CD8+ T cell population, acting as a reservoir to continuously produce effector P1A-specific CD8+ T cells that can then migrate to the tumor. Such a synergistic mechanism would be in line with recent observations showing that a vaccine modality inducing more stem-like CD8+ T cells induced better tumor rejection on PD-1 blockade.[41] However, further studies will be needed to confirm this mechanism in our model.

To support clinical development of our strategy, we evaluated a ChAdOx1/MVA MAGE-A3-NY-ESO-1 in outbred CD1 mice. Though the MAGE-A3 and NY-ESO-1 antigens are xenogeneic in CD1 mice and thus recognized as foreign by the CD1 immune system, it is still useful to validate and demonstrate some key features of the ChAdOx1/MVA MAGE-A3-NY-ESO-1 vaccination strategy. Our results demonstrate that a 'dual antigen prime' with ChAdOx1 encoding both antigens, and a 'single antigen boost' approach with MVA encoding a single antigen could generate very high antigen-specific CD8+ T-cell responses of up to 50% of CD8+ T cells in the blood in some mice. Crucially, we found that the specificity and direction of the response could be tightly controlled by varying the antigen encoded in the MVA

boost after the dual antigen prime. As MAGE-type antigens are expressed differentially in tumors,[9] this strategy allows for preferential targeting of the particular antigens expressed by an individual patient's tumor.

In conclusion, we have shown that ChAdOx1/MVA MAGE vaccination induces potent MAGE-specific CTL responses, promotes CD8^{+} T-cell infiltration in the tumor site and expression of clinically important gene signatures, and improves response to ICB therapy. With these promising data, we will evaluate this cancer vaccine strategy in a clinical trial that will commence shortly.

Author affiliations
[1]Ludwig Institute for Cancer Research, Nuffield Department of Medicine, University of Oxford, Oxford, UK
[2]Département Biologie, Université Claude Bernard Lyon 1, Villeurbanne, Auvergne-Rhône-Alpes, France
[3]Department of Gastroenterology, Peking Union Medical College Hospital, Beijing, China
[4]The Jenner Institute, Nuffield Department of Medicine, University of oxford, Oxford, UK
[5]Ludwig Institute for Cancer Research, WELBIO, de Duve Institute, UCLouvain, Brussels, Belgium

Competing interests IR, AVSH, CSKL, and BJVdE are inventors on a patent that covers viral vectors and methods for the prevention and treatment of cancer. AVSH is a cofounder of and shareholder in Vaccitech Ltd which has supported the MAGE cancer vaccine program and has licensed rights to the ChAdOx1-MVA platform in cancer.

Patient consent for publication Not required.

Ethics approval All animal work was approved by the University of Oxford Animal Care and Ethical Review Committee and experimental procedures were carried out in accordance with the terms of the UK Animals (Scientific Procedures) Act Project Licenses P0D369534 and PB050649E.

Provenance and peer review Not commissioned; externally peer reviewed.

Data availability statement Data are available in a public, open access repository. The gene expression data generated in this study are available at GEO: GSE181111 and GSE181183. The rest of the data are in the Mendeley dataset with DOI: 10.17632/h6rcgfrwry.1

ORCID iDs
Carol Sze Ki Leung http://orcid.org/0000-0002-1545-7228
Benoit J Van den Eynde http://orcid.org/0000-0002-4995-3270

REFERENCES

1 Ribas A, Wolchok JD. Cancer immunotherapy using checkpoint blockade. *Science* 2018;359:1350–5.
2 Hargadon KM, Johnson CE, Williams CJ. Immune checkpoint blockade therapy for cancer: an overview of FDA-approved immune checkpoint inhibitors. *Int Immunopharmacol* 2018;62:29–39.
3 Spranger S, Koblish HK, Horton B, *et al*. Mechanism of tumor rejection with doublets of CTLA-4, PD-1/PD-L1, or IDO blockade involves restored IL-2 production and proliferation of CD8(+) T cells directly within the tumor microenvironment. *J Immunother Cancer* 2014;2:3.
4 Larkin J, Chiarion-Sileni V, Gonzalez R, *et al*. Five-Year survival with combined nivolumab and ipilimumab in advanced melanoma. *N Engl J Med* 2019;381:1535–46.
5 Gandhi L, Rodríguez-Abreu D, Gadgeel S, *et al*. Pembrolizumab plus chemotherapy in metastatic non-small-cell lung cancer. *N Engl J Med* 2018;378:2078–92.
6 Motzer RJ, Tannir NM, McDermott DF, *et al*. Nivolumab plus ipilimumab versus sunitinib in advanced renal-cell carcinoma. *N Engl J Med* 2018;378:1277–90.
7 Tumeh PC, Harview CL, Yearley JH, *et al*. Pd-1 blockade induces responses by inhibiting adaptive immune resistance. *Nature* 2014;515:568–71.
8 Massarelli E, William W, Johnson F, *et al*. Combining immune checkpoint blockade and tumor-specific vaccine for patients with incurable human papillomavirus 16-related cancer: a phase 2 clinical trial. *JAMA Oncol* 2019;5:67–73.
9 Coulie PG, Van den Eynde BJ, van der Bruggen P, *et al*. Tumour antigens recognized by T lymphocytes: at the core of cancer immunotherapy. *Nat Rev Cancer* 2014;14:135–46.
10 Yuan J, Adamow M, Ginsberg BA, *et al*. Integrated NY-ESO-1 antibody and CD8+ T-cell responses correlate with clinical benefit in advanced melanoma patients treated with ipilimumab. *Proc Natl Acad Sci U S A* 2011;108:16723–8.
11 Olsen LR, Tongchusak S, Lin H, *et al*. TANTIGEN: a comprehensive database of tumor T cell antigens. *Cancer Immunol Immunother* 2017;66:731–5.
12 Zhang G, Chitkushev L, Olsen LR, *et al*. TANTIGEN 2.0: a knowledge base of tumor T cell antigens and epitopes. *BMC Bioinformatics* 2021;22:40.
13 Vansteenkiste JF, Cho BC, Vanakesa T, *et al*. Efficacy of the MAGE-A3 cancer immunotherapeutic as adjuvant therapy in patients with resected MAGE-A3-positive non-small-cell lung cancer (MAGRIT): a randomised, double-blind, placebo-controlled, phase 3 trial. *Lancet Oncol* 2016;17:822–35.
14 Dreno B, Thompson JF, Smithers BM, *et al*. Mage-A3 immunotherapeutic as adjuvant therapy for patients with resected, MAGE-A3-positive, stage III melanoma (DERMA): a double-blind, randomised, placebo-controlled, phase 3 trial. *Lancet Oncol* 2018;19:916–29.
15 Brichard VG, Godechal Q. MAGE-A3-specific anticancer immunotherapy in the clinical practice. *Oncoimmunology* 2013;2:e25995.
16 Kruit WHJ, Suciu S, Dreno B, *et al*. Selection of immunostimulant AS15 for active immunization with MAGE-A3 protein: results of a randomized phase II study of the European organisation for research and treatment of cancer melanoma group in metastatic melanoma. *J Clin Oncol* 2013;31:2413–20.
17 Ewer KJ, Lambe T, Rollier CS, *et al*. Viral vectors as vaccine platforms: from immunogenicity to impact. *Curr Opin Immunol* 2016;41:47–54.
18 Antrobus RD, Coughlan L, Berthoud TK, *et al*. Clinical assessment of a novel recombinant simian adenovirus ChAdOx1 as a vectored vaccine expressing conserved influenza A antigens. *Mol Ther* 2014;22:668–74.
19 Cappuccini F, Bryant R, Pollock E, *et al*. Safety and immunogenicity of novel 5T4 viral vectored vaccination regimens in early stage

prostate cancer: a phase I clinical trial. *J Immunother Cancer* 2020;8:e000928.

20 Rühl J, Citterio C, Engelmann C, *et al*. Heterologous prime-boost vaccination protects against EBV antigen-expressing lymphomas. *J Clin Invest* 2019;129:2071–87.

21 Ayers M, Lunceford J, Nebozhyn M, *et al*. IFN-γ-related mRNA profile predicts clinical response to PD-1 blockade. *J Clin Invest* 2017;127:2930–40.

22 Lee JS, Ruppin E. Multiomics prediction of response rates to therapies to inhibit programmed cell death 1 and programmed cell death 1 ligand 1. *JAMA Oncol* 2019;5:1614–8.

23 Brändle D, Bilsborough J, Rülicke T, *et al*. The shared tumor-specific antigen encoded by mouse gene P1A is a target not only for cytolytic T lymphocytes but also for tumor rejection. *Eur J Immunol* 1998;28:4010–9.

24 Uyttenhove C, Godfraind C, Lethé B, *et al*. The expression of mouse gene P1A in testis does not prevent safe induction of cytolytic T cells against a P1A-encoded tumor antigen. *Int J Cancer* 1997;70:349–56.

25 Boon T, Van den Eynde B, Hirsch H, *et al*. Genes coding for tumor-specific rejection antigens. *Cold Spring Harb Symp Quant Biol* 1994;59:617–22.

26 Leung CS, Maurer MA, Meixlsperger S, *et al*. Robust T-cell stimulation by Epstein-Barr virus-transformed B cells after antigen targeting to DEC-205. *Blood* 2013;121:1584–94.

27 Halbroth BR, Sebastian S, Poyntz HC, *et al*. Development of a Molecular Adjuvant to Enhance Antigen-Specific CD8⁺ T Cell Responses. *Sci Rep* 2018;8:15020.

28 Biswas S, Dicks MDJ, Long CA, *et al*. Transgene optimization, immunogenicity and in vitro efficacy of viral vectored vaccines expressing two alleles of Plasmodium falciparum AMA1. *PLoS One* 2011;6:e20977.

29 Van den Eynde B, Lethé B, Van Pel A, *et al*. The gene coding for a major tumor rejection antigen of tumor P815 is identical to the normal gene of syngeneic DBA/2 mice. *J Exp Med* 1991;173:1373–84.

30 Cappuccini F, Stribbling S, Pollock E, *et al*. Immunogenicity and efficacy of the novel cancer vaccine based on simian adenovirus and MVA vectors alone and in combination with PD-1 mAb in a mouse model of prostate cancer. *Cancer Immunol Immunother* 2016;65:701–13.

31 Mosely SIS, Prime JE, Sainson RCA, *et al*. Rational selection of syngeneic preclinical tumor models for immunotherapeutic drug discovery. *Cancer Immunol Res* 2017;5:29–41.

32 Youn J-I, Kumar V, Collazo M, *et al*. Epigenetic silencing of retinoblastoma gene regulates pathologic differentiation of myeloid cells in cancer. *Nat Immunol* 2013;14:211–20.

33 Cristescu R, Mogg R, Ayers M, *et al*. Pan-tumor genomic biomarkers for PD-1 checkpoint blockade-based immunotherapy. *Science* 2018;362:eaar3593.

34 Juneja VR, McGuire KA, Manguso RT, *et al*. Pd-L1 on tumor cells is sufficient for immune evasion in immunogenic tumors and inhibits CD8 T cell cytotoxicity. *J Exp Med* 2017;214:895–904.

35 Wherry EJ, Kurachi M. Molecular and cellular insights into T cell exhaustion. *Nat Rev Immunol* 2015;15:486–99.

36 Tirosh I, Izar B, Prakadan SM, *et al*. Dissecting the multicellular ecosystem of metastatic melanoma by single-cell RNA-seq. *Science* 2016;352:189–96.

37 Scott AC, Dündar F, Zumbo P, *et al*. Tox is a critical regulator of tumour-specific T cell differentiation. *Nature* 2019;571:270–4.

38 Miller BC, Sen DR, Al Abosy R, *et al*. Subsets of exhausted CD8⁺ T cells differentially mediate tumor control and respond to checkpoint blockade. *Nat Immunol* 2019;20:326–36.

39 Sade-Feldman M, Yizhak K, Bjorgaard SL, *et al*. Defining T cell states associated with response to checkpoint immunotherapy in melanoma. *Cell* 2018;175:e20:998–1013.

40 Krishna S, Lowery FJ, Copeland AR, *et al*. Stem-Like CD8 T cells mediate response of adoptive cell immunotherapy against human cancer. *Science* 2020;370:1328–34.

41 Baharom F, Ramirez-Valdez RA, Tobin KKS, *et al*. Intravenous nanoparticle vaccination generates stem-like TCF1⁺ neoantigen-specific CD8⁺ T cells. *Nat Immunol* 2021;22:41–52.

42 Im SJ, Hashimoto M, Gerner MY, *et al*. Defining CD8+ T cells that provide the proliferative burst after PD-1 therapy. *Nature* 2016;537:417–21.

43 Näslund TI, Uyttenhove C, Nordström EKL, *et al*. Comparative prime-boost vaccinations using Semliki Forest virus, adenovirus, and ALVAC vectors demonstrate differences in the generation of a protective central memory CTL response against the P815 tumor. *J Immunol* 2007;178:6761–9.

44 Bonilla WV, Kirchhammer N, Marx A-F, *et al*. Heterologous arenavirus vector prime-boost overrules self-tolerance for efficient tumor-specific CD8 T cell attack. *Cell Rep Med* 2021;2:100209.

45 Harlin H, Meng Y, Peterson AC, *et al*. Chemokine expression in melanoma metastases associated with CD8+ T-cell recruitment. *Cancer Res* 2009;69:3077–85.

46 Mikucki ME, Fisher DT, Matsuzaki J, *et al*. Non-Redundant requirement for CXCR3 signalling during tumoricidal T-cell trafficking across tumour vascular checkpoints. *Nat Commun* 2015;6:7458.

47 Romero JM, Grünwald B, Jang G-H, *et al*. A Four-Chemokine signature is associated with a T-cell-Inflamed phenotype in primary and metastatic pancreatic cancer. *Clin Cancer Res* 2020;26:1997–2010.

48 Im SJ, Konieczny BT, Hudson WH, *et al*. PD-1+ stemlike CD8 T cells are resident in lymphoid tissues during persistent LCMV infection. *Proc Natl Acad Sci U S A* 2020;117:4292–9.

49 Lugli E, Dominguez MH, Gattinoni L, *et al*. Superior T memory stem cell persistence supports long-lived T cell memory. *J Clin Invest* 2013;123:594–9.

50 Siddiqui I, Schaeuble K, Chennupati V, *et al*. Intratumoral Tcf1⁺PD-1⁺CD8⁺ T Cells with Stem-like Properties Promote Tumor Control in Response to Vaccination and Checkpoint Blockade Immunotherapy. *Immunity* 2019;50:e10:195–211.